

Stau relic density at the Big-Bang nucleosynthesis era consistent with the abundance of the light element nuclei in the coannihilation scenario

Toshifumi Jittoh,¹ Kazunori Kohri,^{2,3} Masafumi Koike,¹ Joe Sato,¹ Takashi Shimomura,^{4,5} and Masato Yamanaka⁶

¹*Department of Physics, Saitama University, Shimo-okubo, Sakura-ku, Saitama, 338-8570, Japan*

²*Physics Department, Lancaster University LA1 4YB, UK*

³*Department of Physics, Tohoku University, Sendai 980-8578, Japan*

⁴*Departament de Física Teòrica and IFIC, Universitat de València-CSIC, E-46100 Burjassot, València, Spain*

⁵*Yukawa Institute for Theoretical Physics, Kyoto University, Kyoto 606-8502, Japan*

⁶*Institute for Cosmic Ray Research, University of Tokyo, Kashiwa 277-8582, Japan*

We calculate the relic density of stau at the beginning of the Big-Bang Nucleosynthesis (BBN) era in the coannihilation scenario of minimal supersymmetric standard model (MSSM). In this scenario, stau can be long-lived and form bound states with nuclei. We put constraints on the parameter space of MSSM by connecting the calculation of the relic density of stau to the observation of the light elements abundance, which strongly depends on the relic density of stau. Consistency between the theoretical prediction and the observational result, both of the dark matter abundance and the light elements abundance, requires the mass difference between the lighter stau and the lightest neutralino to be around 100MeV, the stau mass to be 300 – 400 GeV, and the mixing angle of the left and right-handed staus to be $\sin \theta_\tau = (0.65 - 1)$.

I. INTRODUCTION

Cosmological observations have established the existence of the non-baryonic dark matter (DM) [1]. These observations suggest that the DM is a stable and weakly-interacting particle with a mass of $\mathcal{O}(100)$ GeV. Many hypothetical candidates for the DM have been proposed in models of particle physics beyond the standard model (SM), and one of the most attractive candidates is the lightest neutralino, $\tilde{\chi}^0$, in supersymmetric extensions of the SM with R parity conservation. Neutralino is a linear combination of the superpartners of $U(1)$, $SU(2)$ gauge bosons and the two neutral Higgses, and is stable when it is the lightest supersymmetric particle (LSP). Indeed it accounts for the observed DM abundance when it is degenerate in mass to the next lightest supersymmetric particle (NLSP) and hence coannihilates with the NLSP [2]. We consider the setup that the LSP is a neutralino consisting of mainly bino, the superpartner of $U(1)$ gauge boson, and the NLSP is the lighter stau, the superpartner of tau lepton. This is naturally realized in the MSSM with the unification condition at the grand unified theory scale. The minimal supersymmetric SM (MSSM) has two eigenstates of stau as physical state. In absence of inter-generational mixing the mass eigenstate of stau is given by the linear combination of the left-handed stau $\tilde{\tau}_L$ and the right-handed stau $\tilde{\tau}_R$ as

$$\tilde{\tau} = \cos \theta_\tau \tilde{\tau}_L + \sin \theta_\tau e^{-i\gamma_\tau} \tilde{\tau}_R, \quad (1)$$

where θ_τ is the left-right mixing angle and γ_τ is the CP violating phase.

In a scenario of the coannihilation, the NLSP stau can be long-lived if the mass difference, δm , between neutralino and stau is small enough to forbid two-body decays of stau into neutralino. It was shown in [3] that the

lifetime of stau is longer than 1000 second for $\delta m \lesssim 100$ MeV. It is known [4–18] that the long-lived charged particles affect the relic abundance of the light nuclei during or after the big-bang nucleosynthesis (BBN).

There is a discrepancy, the so-called ${}^7\text{Li}$ problem, on the primordial ${}^7\text{Li}$ abundance between the prediction from the standard BBN (SBBN) and the observations [19, 20]. Combined with the up-to-date values of baryon-to-photon ratio, $\eta = (6.225 \pm 0.170) \times 10^{-10}$ from Wilkinson Microwave Anisotropy Probe (WMAP) [1], the SBBN predicts the ${}^7\text{Li}$ to proton ratio, $({}^7\text{Li}/\text{H})_{\text{SBBN}} = 5.24_{-0.67}^{+0.71} \times 10^{-10}$, which is by about four-times larger than its observed value in poor-metal halos [19, 21]. Because there exists no general agreements about astrophysical scenarios to reduce the ${}^7\text{Li}$ abundance [22–25], it is natural to consider nonstandard effects.

The authors have investigated the BBN including the long-lived stau [14, 15]. The long-lived stau form a bound state with nuclei ($\tilde{\tau}N$), and consequently convert it into a nucleus with a smaller atomic number. Here N stands for a nucleus. In this scenario, the abundance of ${}^7\text{Li}$ is reduced through the conversion process, $(\tilde{\tau}{}^7\text{Be}) \rightarrow \tilde{\chi}^0 + \nu_\tau + {}^7\text{Li}$ and the further destruction of ${}^7\text{Li}$ by either a collision with a background proton or another conversion process, $(\tilde{\tau}{}^7\text{Li}) \rightarrow \tilde{\chi}^0 + \nu_\tau + {}^7\text{He}$. Therefore, the more these bound states are formed, the more the ${}^7\text{Li}$ abundance is reduced. The number density of the bound state is determined by the relic density of stau. In [14, 15], we assumed $Y_{\tilde{\tau},\text{FO}}$ and δm to be free parameters of the scenario, where $Y_{\tilde{\tau},\text{FO}}$ is the yield value of stau at the time of decoupling from the thermal bath. The full calculation of the light nucleus abundances showed a region in $(\delta m, Y_{\tilde{\tau},\text{FO}})$ plane where the ${}^7\text{Li}$ problem is solved consistently with the observational constraints on the other nuclei. The region points $Y_{\tilde{\tau},\text{FO}}$ to be close to

the yield value of the DM and δm to be around 0.1 GeV, respectively.

In this work, we improve our previous analysis by calculating $Y_{\tilde{\tau}, \text{FO}}$ with taking the relic abundance of DM into account. The outline of this paper is as follows. In section II, we review the formalism for the calculation of the relic density of stau, and derive the Boltzmann equations of stau and neutralino for the calculation. In section III, we present the numerical results of the calculation, and prove the parameter space for solving the ^7Li problem. Section IV is devoted to a summary and discussion.

II. FORMALISM FOR THE CALCULATION OF RELIC DENSITY OF STAU AT THE BBN ERA

In this section, we prepare to calculate the relic density of stau at the BBN era. Firstly, in subsection II A, we briefly review the Boltzmann equations for the number density of stau and neutralino based on the thermal relic scenario. Then, in subsection II B, we discuss the number density evolution of stau and neutralino quantitatively. In subsection II C, we investigate the significant processes for the calculation of the relic density of stau. Finally, we obtain the Boltzmann equations for the relic density of stau in a convenient form.

A. Boltzmann equations for the number density evolution of stau and neutralino

In this subsection, we show the Boltzmann equations of stau and neutralino and briefly review their quantitative structure based on [26] (see also a recent paper[27]).

We are interested in the relic density of stau in the coannihilation scenario. In this scenario, stau and neutralino are quasi-degenerate in mass and decouple from the thermal bath almost at the same time [2]. Thus the relic density of stau is given by solving a coupled set of the Boltzmann equations for stau and neutralino as simultaneous differential equation. For simplicity, we use the Maxwell-Boltzmann statistics for all species instead of the Fermi-Dirac for fermions and the Bose-Einstein for bosons, and assume T invariance. With these simplifications, the Boltzmann equations of them are given as follows

$$\begin{aligned} \frac{dn_{\tilde{\tau}^+}}{dt} + 3Hn_{\tilde{\tau}^+} = & - \sum_i \sum_{X,Y} \langle \sigma v \rangle_{\tilde{\tau}^+ i \leftrightarrow XY} \left[n_{\tilde{\tau}^+} n_i - n_{\tilde{\tau}^+}^{eq} n_i^{eq} \left(\frac{n_X n_Y}{n_X^{eq} n_Y^{eq}} \right) \right] \\ & - \sum_{i \neq \tilde{\tau}^+} \sum_{X,Y} \left\{ \langle \sigma' v \rangle_{\tilde{\tau}^+ X \rightarrow iY} \left[n_{\tilde{\tau}^+} n_X \right] - \langle \sigma' v \rangle_{iY \rightarrow \tilde{\tau}^+ X} \left[n_i n_Y \right] \right\} \end{aligned} \quad (2)$$

$$\begin{aligned} \frac{dn_{\tilde{\chi}}}{dt} + 3Hn_{\tilde{\chi}} = & - \sum_i \sum_{X,Y} \langle \sigma v \rangle_{\tilde{\chi} i \leftrightarrow XY} \left[n_{\tilde{\chi}} n_i - n_{\tilde{\chi}}^{eq} n_i^{eq} \left(\frac{n_X n_Y}{n_X^{eq} n_Y^{eq}} \right) \right] \\ & - \sum_{i \neq \tilde{\chi}} \sum_{X,Y} \left\{ \langle \sigma' v \rangle_{\tilde{\chi} X \rightarrow iY} \left[n_{\tilde{\chi}} n_X \right] - \langle \sigma' v \rangle_{iY \rightarrow \tilde{\chi} X} \left[n_i n_Y \right] \right\} \end{aligned} \quad (3)$$

$$\begin{aligned} \frac{dn_{\tilde{\tau}^-}}{dt} + 3Hn_{\tilde{\tau}^-} = & - \sum_i \sum_{X,Y} \langle \sigma v \rangle_{\tilde{\tau}^- i \leftrightarrow XY} \left[n_{\tilde{\tau}^-} n_i - n_{\tilde{\tau}^-}^{eq} n_i^{eq} \left(\frac{n_X n_Y}{n_X^{eq} n_Y^{eq}} \right) \right] \\ & - \sum_{i \neq \tilde{\tau}^-} \sum_{X,Y} \left\{ \langle \sigma' v \rangle_{\tilde{\tau}^- X \rightarrow iY} \left[n_{\tilde{\tau}^-} n_X \right] - \langle \sigma' v \rangle_{iY \rightarrow \tilde{\tau}^- X} \left[n_i n_Y \right] \right\} \end{aligned} \quad (4)$$

Here n and n^{eq} represent the actual number density and the equilibrium number density of each particle, and H is the Hubble expansion rate. Index i denotes stau and neutralino, and indices X and Y denote SM particles. Note that if relevant SM particles are in thermal equilibrium, $n_X = n_X^{eq}$, $n_Y = n_Y^{eq}$, and $(n_X n_Y / n_X^{eq} n_Y^{eq}) = 1$ then these equations are reduced into a familiar form. $\langle \sigma v \rangle$ and $\langle \sigma' v \rangle$ are the thermal averaged cross sections, which is defined by

$$\begin{aligned} \langle \sigma v \rangle_{12 \rightarrow 34} & \equiv g_{12} \frac{\int d^3 \mathbf{p}_1 d^3 \mathbf{p}_2 f_1 f_2 (\sigma v)_{12 \rightarrow 34}}{\int d^3 \mathbf{p}_1 d^3 \mathbf{p}_2 f_1 f_2} \\ & = g_{12} \frac{\int d^3 \mathbf{p}_1 d^3 \mathbf{p}_2 f_1 f_2 (\sigma v)_{12 \rightarrow 34}}{n_1^{eq} n_2^{eq}}, \end{aligned} \quad (5)$$

where f is the distribution function of a particle, v is the relative velocity between initial state particles, and $g_{12} = 2(1)$ for same (different) particles 1 and 2. In this work, we assume that all of the supersymmetric particles except for stau and neutralino are heavy, and therefore do not involve them in the coannihilation processes.

The first line on the right-hand side of Eqs. (2), (3), and (4) accounts for the annihilation and the inverse annihilation processes of the supersymmetric particles ($ij \leftrightarrow XY$). Here index j denotes stau and neutralino. As long as the R-parity is conserved, as shown later, the final number density of neutralino DM is controlled only by these processes. The second line accounts for the exchange processes by scattering off the cosmic thermal background ($iX \leftrightarrow jY$). These processes exchange stau with neutralino and vice versa, and thermalize them. Consequently, the number density ratio between them is controlled by these processes. Instead, these processes leave the total number density of the supersymmetric particles. Note that in general, although there are terms which account for decay and inverse decay processes of stau ($\tilde{\tau} \leftrightarrow \tilde{\chi} XY \dots$) in the Boltzmann equations, we omit them. It is because we are interested in solving the ^7Li

problem by the long-lived stau, and the whole intention of this work is to search parameters which can provide the solution for the ${}^7\text{Li}$ problem. Hence we assume that the stau is stable enough to survive until the BBN era, and focusing on the mass difference between stau and neutralino is small enough to make it possible.

B. The evolution of the number density of stau and neutralino

In this subsection, we discuss the evolution of the number density of each species. Firstly, we discuss the number density evolution of neutralino DM. Since we have assumed R-parity conservation, all of the supersymmetric particles eventually decay into the LSP neutralino. Thus its final number density is simply described by the sum of the number density of all the supersymmetric particles :

$$N = \sum_i n_i . \quad (6)$$

For N , that is the number density of the neutralino, we get the Boltzmann equation by summing up Eqs. (2), (3), and (4),

$$\frac{dN}{dt} + 3HN = -\langle\sigma v\rangle_{sum} \left[NN - N^{eq}N^{eq} \right] \quad (7)$$

$$\langle\sigma v\rangle_{sum} \equiv \sum_{i=\tilde{\chi}, \tilde{\tau}} \sum_{X, Y} \langle\sigma v\rangle_{\tilde{\chi}i \leftrightarrow XY} . \quad (8)$$

Notice that the terms describing the exchange processes in each Boltzmann equations cancel each other out. Solving the Eq. (7), we obtain N and find the freeze out temperature of the total number density of all the supersymmetric particles T_f by using the standard technique [26]:

$$\frac{m_{\tilde{\chi}}}{T_f} = \ln \frac{0.038 g m_{pl} m_{\tilde{\chi}} \langle\sigma v\rangle}{g_*^{1/2} (m_{\tilde{\chi}}/T_f)} \simeq 25 . \quad (9)$$

Here, g and $m_{\tilde{\chi}}$ are the internal degrees of freedom and the mass of neutralino, respectively. The Planck mass $m_{pl} = 1.22 \times 10^{19}$ GeV, and g_* are the total number of the relativistic degrees of freedom. Consequently, we see that $4 \text{ GeV} \lesssim T_f \lesssim 40 \text{ GeV}$ for $100 \text{ GeV} \lesssim m_{\tilde{\chi}} \lesssim 1000 \text{ GeV}$.

Now we will discuss the number density evolution of stau. To obtain the relic density of stau, we solve a coupled set of the Boltzmann equations, (2), (3), and (4), as simultaneous differential equation. Each Boltzmann equation contains the contributions of the exchange processes. These processes exchange stau with neutralino and vice versa. At the temperature T_f , the interaction rate of the exchange processes is much larger than that of the annihilation and the inverse annihilation processes.

This is because the cross sections of the exchange processes are in the same order of magnitude as that of the annihilation and the inverse annihilation, but the number density of the SM particles is much larger than that of the supersymmetric particles which is suppressed by the Boltzmann factor. Thus even if the total number density of stau and neutralino is frozen out at the temperature T_f , each number density of them continue to evolve through the exchange processes.

Thus, to calculate the relic density of stau, we have to follow the two-step procedures. As a first step, we calculate the total relic density of the supersymmetric particles by solving the Eq. (7). We use the publicly available program micrOMEGAs [28] to calculate it. The second step is the calculation of the number density ratio of stau and neutralino. The second step is significant for calculating the relic density of stau at the BBN era, and hence we will discuss it in detail in the next subsection.

C. The exchange processes and Lagrangian for describing them

After the freeze-out of the total number density of stau and neutralino, each of them is exchanged through the following processes

$$\begin{aligned} \tilde{\tau}\gamma &\longleftrightarrow \tilde{\chi}\tau \\ \tilde{\chi}\gamma &\longleftrightarrow \tilde{\tau}\tau . \end{aligned} \quad (10)$$

Notice that although there are other exchange processes via weak interaction (for example, $\tilde{\tau}W \leftrightarrow \tilde{\chi}\nu_\tau$, $\tilde{\tau}\nu_\tau \leftrightarrow \tilde{\chi}W$, and so on), we can omit them. This is because the number density of W boson is not enough to work these processes sufficiently due to the Boltzmann factor suppression, and the final state W boson is kinematically forbidden when the thermal bath temperature is less than T_f . These processes (Eq. (10)) are described by the Lagrangian

$$\mathcal{L} = \tilde{\tau}^* \overline{\tilde{\chi}^0} (g_L P_L + g_R P_R) \tau - ie(\tilde{\tau}^* (\partial_\mu \tilde{\tau}) - (\partial_\mu \tilde{\tau}^*) \tilde{\tau}) A^\mu + \text{h.c.}, \quad (11)$$

where e is the electromagnetic coupling constant, P_L and P_R are the projection operators, and $l \in \{e, \mu\}$. g_L and g_R are the coupling constants, given by

$$\begin{aligned} g_L &= \frac{g}{\sqrt{2} \cos \theta_W} \sin \theta_W \cos \theta_\tau, \\ g_R &= \frac{\sqrt{2}g}{\cos \theta_W} \sin \theta_W \sin \theta_\tau e^{i\gamma_\tau}, \end{aligned} \quad (12)$$

where g is the $SU(2)_L$ gauge coupling constant, and θ_W is the Weinberg angle.

The evolution of the stau number density is governed only by the exchange processes (Eq.(10)) after the freeze-out of the total relic density of stau and neutralino. When we calculate it, we should pay attention to two essential points relevant to the exchange processes.

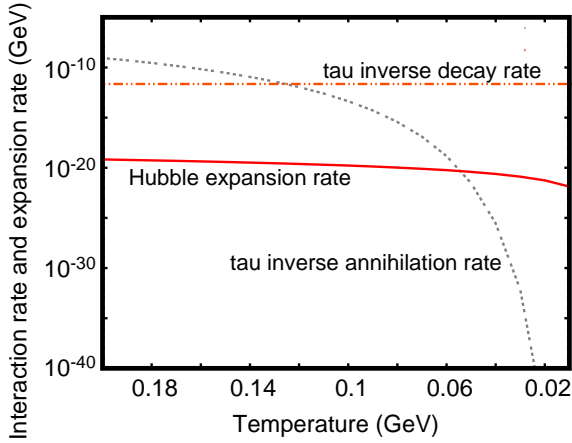


FIG. 1: The inverse annihilation rate of tau leptons $\langle\Gamma\rangle n_X^{eq}$, the inverse decay rate of tau leptons $\langle\Gamma\rangle$, and the Hubble expansion rate H as a function of the thermal bath temperature.

One is the competition between the interaction rate of the exchange processes and the Hubble expansion rate, since when these interaction rates get smaller than the Hubble expansion rate, the relic density of stau would be frozen out. The other is whether tau leptons are in the thermal bath or not. The interaction rate of the exchange processes strongly depends on the number density of tau leptons. When tau leptons are in the thermal bath, the number density ratio between stau and neutralino are given by the thermal ratio,

$$\frac{n_{\tilde{\tau}}}{n_{\chi}} \simeq \frac{e^{-m_{\tilde{\tau}}/T}}{e^{-m_{\tilde{\chi}}/T}} = \exp\left(-\frac{\delta m}{T}\right), \quad (13)$$

through the exchange processes. On the contrary, once tau leptons decouple from the thermal bath, the ratio cannot reach this value. To calculate the relic density of stau, we have to comprehend the temperature of tau lepton decoupling.

To see whether tau leptons are in the thermal bath or not, we consider the Boltzmann equation for its number density, n_{τ} ,

$$\frac{dn_{\tau}}{dt} + 3Hn_{\tau} = -\langle\sigma v\rangle \left[n_{\tau}n_X - n_{\tau}^{eq}n_X^{eq} \left(\frac{n_Y n_Z}{n_Y^{eq} n_Z^{eq}} \right) \right] - \langle\Gamma\rangle \left[n_{\tau} - n_{\tau}^{eq} \left(\frac{n_X n_Y \dots}{n_X^{eq} n_Y^{eq} \dots} \right) \right], \quad (14)$$

$$\langle\sigma v\rangle = \sum_{X,Y,Z} \langle\sigma v\rangle_{\tau X \leftrightarrow Y Z}, \quad \langle\Gamma\rangle = \sum_{X,Y,\dots} \langle\Gamma\rangle_{\tau \leftrightarrow X Y \dots}, \quad (15)$$

where indices X , Y , and Z denote the SM particles, and $\langle\Gamma\rangle$ represents the thermal averaged decay rate

of tau lepton. When the SM particles X , Y , and Z are in the thermal equilibrium, $(n_Y n_Z)/(n_Y^{eq} n_Z^{eq}) = (n_X n_Y \dots)/(n_X^{eq} n_Y^{eq} \dots) = 1$, and hence tau leptons are sufficiently produced through the inverse annihilation and/or the inverse decay processes as long as these interaction rates are larger than the Hubble expansion rate. Therefore, whether tau leptons are in the thermal bath or not can be distinguished by comparing the Hubble expansion rate H with the inverse annihilation rate of tau lepton $\langle\sigma v\rangle n_X^{eq}$, and the inverse decay rate of tau lepton $\langle\Gamma\rangle$. In other words, the inequality expression

$$\langle\sigma v\rangle n_X^{eq} > H \quad \text{and/or} \quad \langle\Gamma\rangle > H \quad (16)$$

indicates that tau leptons are in the thermal bath. Fig. 1 shows $\langle\Gamma\rangle n_X^{eq}$, $\langle\Gamma\rangle$, and H as a function of the thermal bath temperature. As shown in Fig. 1, the inverse decay rate of tau lepton is much larger than the Hubble expansion rate. Thus, we can conclude that tau leptons remain in the thermal bath still at the beginning of BBN.

D. Calculation of the number density ratio of stau and neutralino

We are now in a position to calculate the number density ratio of stau and neutralino. In this subsection, we will show a set of relevant Boltzmann equations.

The right-hand side of the Boltzmann equations (Eqs. (2), (3), and (4)) depends only on temperature, and hence it is convenient to use temperature T instead of time t as independent variable. To do this, we reformulate the Boltzmann equations by using the ratio of the number density to the entropy density s :

$$Y_i = \frac{n_i}{s}. \quad (17)$$

Consequently, we obtain the Boltzmann equations for the number density evolution of stau and neutralino

$$\frac{dY_{\tilde{\tau}^-}}{dT} = \left[3HTg_*(T) \right]^{-1} \left[3g_*(T) + T \frac{dg_*(T)}{dT} \right] s \times \left\{ \langle\sigma v\rangle_{\tilde{\tau}^- \gamma \rightarrow \tilde{\chi} \tau^-} Y_{\tilde{\tau}^-} Y_{\gamma} - \langle\sigma v\rangle_{\tilde{\chi} \tau^- \rightarrow \tilde{\tau}^- \gamma} Y_{\tilde{\chi}} Y_{\tau^-} + \langle\sigma v\rangle_{\tilde{\tau}^- \tau^+ \rightarrow \tilde{\chi} \gamma} Y_{\tilde{\tau}^-} Y_{\tau^+} - \langle\sigma v\rangle_{\tilde{\chi} \tau^+ \rightarrow \tilde{\tau}^- \tau^+} Y_{\tilde{\chi}} Y_{\gamma} \right\} \quad (18)$$

$$\frac{dY_{\tilde{\tau}^+}}{dT} = \left[3HTg_*(T) \right]^{-1} \left[3g_*(T) + T \frac{dg_*(T)}{dT} \right] s \times \left\{ \langle\sigma v\rangle_{\tilde{\tau}^+ \gamma \rightarrow \tilde{\chi} \tau^+} Y_{\tilde{\tau}^+} Y_{\gamma} - \langle\sigma v\rangle_{\tilde{\chi} \tau^+ \rightarrow \tilde{\tau}^+ \gamma} Y_{\tilde{\chi}} Y_{\tau^+} + \langle\sigma v\rangle_{\tilde{\tau}^+ \tau^- \rightarrow \tilde{\chi} \gamma} Y_{\tilde{\tau}^+} Y_{\tau^-} - \langle\sigma v\rangle_{\tilde{\chi} \tau^- \rightarrow \tilde{\tau}^+ \tau^+} Y_{\tilde{\chi}} Y_{\gamma} \right\} \quad (19)$$

$$\begin{aligned}
\frac{dY_{\tilde{\chi}}}{dT} = & \left[3HTg_*(T) \right]^{-1} \left[3g_*(T) + T \frac{dg_*(T)}{dT} \right] s \\
& \times \left\{ \langle \sigma v \rangle_{\tilde{\chi}\tau^- \rightarrow \tilde{\tau}^-\gamma} Y_{\tilde{\chi}} Y_{\tau^-} - \langle \sigma v \rangle_{\tilde{\tau}^-\gamma \rightarrow \tilde{\chi}\tau^-} Y_{\tilde{\tau}^-} Y_{\gamma} \right. \\
& + \langle \sigma v \rangle_{\tilde{\chi}\gamma \rightarrow \tilde{\tau}^-\tau^+} Y_{\tilde{\chi}} Y_{\gamma} - \langle \sigma v \rangle_{\tilde{\tau}^-\tau^+ \rightarrow \tilde{\chi}\gamma} Y_{\tilde{\tau}^-} Y_{\tau^+} \\
& + \langle \sigma v \rangle_{\tilde{\chi}\tau^+ \rightarrow \tilde{\tau}^+\gamma} Y_{\tilde{\chi}} Y_{\tau^+} - \langle \sigma v \rangle_{\tilde{\tau}^+\gamma \rightarrow \tilde{\chi}\tau^+} Y_{\tilde{\tau}^+} Y_{\gamma} \\
& \left. + \langle \sigma v \rangle_{\tilde{\chi}\gamma \rightarrow \tilde{\tau}^+\tau^-} Y_{\tilde{\chi}} Y_{\gamma} - \langle \sigma v \rangle_{\tilde{\tau}^+\tau^- \rightarrow \tilde{\chi}\gamma} Y_{\tilde{\tau}^+} Y_{\tau^-} \right\}. \tag{20}
\end{aligned}$$

Here $g_*(T)$ is the relativistic degrees of freedom, and we use

$$s = \frac{2\pi^2}{45} g_*(T) T^3, \quad H = 1.66 g_*^{1/2} \frac{T^2}{m_{pl}}. \tag{21}$$

We obtain the relic density of stau at the BBN era by integrating these equations from T_f to the temperature for beginning the BBN under the initial condition of the total number density of stau and neutralino. These equations make it clear that if the tau number density is out of the equilibrium, the ratio between those of stau and neutralino does not satisfy the Eq.(13).

III. NUMERICAL RESULTS

In this section, we will first show the evolution of the stau number density, and then study the relation between the relic density of stau and the modification of nucleosynthesis. Finally, we study a solution of the ^7Li problem with long-lived stau in the coannihilation scenario based on Ref. [14–16].

A. Total abundance

As a first step for the calculation of the relic number density of stau, based on the discussion in section II B, we calculate the total abundance of stau and neutralino with micrOMEGAs [28]. Fig. 2 shows the total abundance, which corresponds to the relic abundance of DM, as a function of $\sin \theta_\tau$, where θ_τ is the mixing angle between left and right-handed stau. Each curved line shows the total abundance for each stau mass, and horizontal band represents the allowed region from the WMAP observation at the 3σ level ($0.0913 \leq \Omega_{DM} h^2 \leq 0.1285$), and the region inside the horizontal dotted lines corresponds to allowed region at the 2σ level ($0.0963 \leq \Omega_{DM} h^2 \leq 0.1213$) [1]. In the left side of vertical lines, the LSP is the left-handed sneutrino. Three lines correspond to $m_{\tilde{\tau}} = 400, 350, 300$ GeV from left to right. Since the left-handed sneutrino DM has been ruled out by constraints from the direct detection experiments [29], we focus on the right-side region. Here we took $\gamma_\tau = 0$ and $\delta m = 100$ MeV.

The total abundance increases first as the heavier stau mixes to the lighter stau, then turns to decrease at

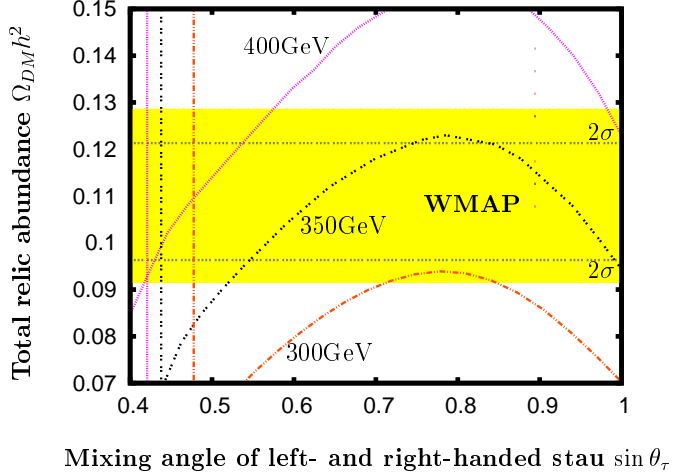


FIG. 2: Total abundance of staus and neutralinos, which corresponds to the relic abundance of DM. Each line shows the total abundance, and attached value represents the stau mass. Yellow band represents the allowed region from the WMAP observation at the 3σ level, and the region inside the horizontal dotted lines corresponds to allowed region at the 2σ level [1]. In the left side of vertical lines, the LSP is left-handed sneutrino. Three lines correspond to $m_{\tilde{\tau}} = 400, 350, 300$ GeV from left to right.

$\sin \theta_\tau \simeq 0.8$. The increase of the abundance can be understood by the fact that the annihilation cross section of $\tilde{\tau} + \tilde{\tau} \rightarrow \tau + \tau$ becomes smaller as the heavier stau mixes. The increase is gradually compensated by two annihilation processes, $\tilde{\tau} + \tilde{\tau}^* \rightarrow W^+ + W^-$ and $\tilde{\chi}_1^0 + \tilde{\tau} \rightarrow W^- + \nu_\tau$, as the left-right mixing becomes large. The latter process can not be ignored because left-handed sneutrino is degenerate to stau and neutralino in the present parameter set. These processes become significant for $\sin \theta_\tau < 0.8$. Another process which reduces the total abundance due to the left-right mixing is $\tilde{\tau} + \tilde{\tau}^* \rightarrow t + \bar{t}$ through s-channel exchange of the heavy Higgses. This annihilation process becomes significant as the mixing reaches to $\pi/4$ and the masses of two staus are split. In fig. 2, the mass difference between the lighter and the heavier stau is fixed to be 30 GeV to maximize the DM abundance, but the same result can be obtained by changing the stau mass for another values of the mass difference. As shown in Fig. 2, the total abundance also strongly depends on $m_{\tilde{\tau}}$. This is understood as follows. In the non-relativistic limit, since the relic number density of relic species is proportional to $(m_{relic} \langle \sigma v \rangle_{sum})^{-1}$ and $\langle \sigma v \rangle_{sum}$ (Eq. (8)) is proportional to $1/m_{relic}^2$ [30], the total number density N is proportional to $m_{\tilde{\tau}}$,

$$N \propto \frac{1}{m_{\tilde{\tau}} \langle \sigma v \rangle_{sum}} \propto \frac{1}{1/m_{\tilde{\tau}}} = m_{\tilde{\tau}}, \tag{22}$$

and the total abundance is given by $\Omega_{DM} h^2 \sim m_{\tilde{\tau}} N$. Thus the total abundance is proportional to $m_{\tilde{\tau}}^2$, and it is consistent with the result in Fig. 2.

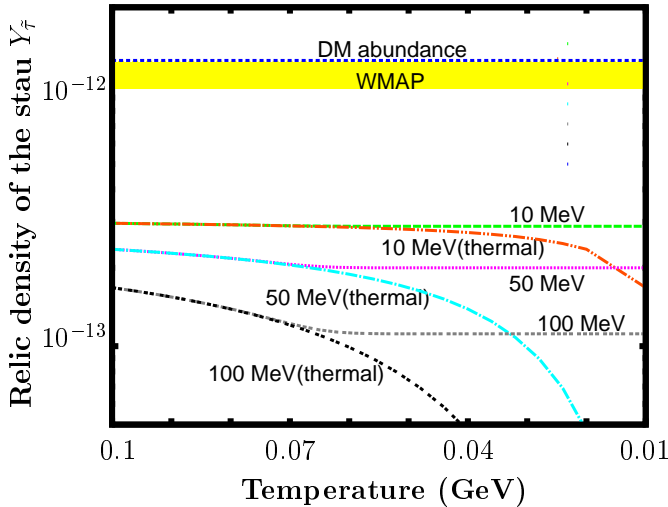


FIG. 3: The evolution of the number density of negative charged stau. Each line attached $[\delta m]$ shows the actual evolution of the number density of stau, while the one attached $[\delta m(\text{thermal})]$ shows its evolution under the equilibrium determined given by Eq. (13) and the total relic abundance. Yellow band represents the allowed region from the WMAP observation at the 2σ level [1].

B. Stau relic density at the BBN era

Next, we solve the Boltzmann equations (18), (19), and (20) numerically, and obtain the ratio of the stau number density to the total number density of stau and neutralino. Fig. 3 shows the evolution of the number density of stau as a function of the universe temperature. Here we took $m_{\tilde{\tau}} = 350$ GeV, $\sin \theta_{\tau} = 0.8$, and $\gamma_{\tau} = 0$ and chose $\delta m = 10$ MeV, 50 MeV, and 100 MeV as sample points. Each line attached $[\delta m]$ shows the actual evolution of the number density of stau, while the one attached $[\delta m(\text{thermal})]$ shows its evolution under the equilibrium determined by Eq. (13) and the total relic abundance. Horizontal dotted line represents the relic density of DM, which is the total abundance calculated above. We took it as a initial condition of total value for the calculation of the number density ratio. Yellow band represents the allowed region from the WMAP observation at the 2σ level [1].

The number density evolution of stau is qualitatively understood as follows. As shown in Fig. 3, the freeze-out temperature of stau almost does not depend on δm . It is determined by the exchange processes Eq. (10), whose magnitude $\langle \sigma v \rangle Y_{\tilde{\tau}} Y_{\gamma}$ is governed by the factor $e^{-(m_{\tau} - \delta m)/T}$, where m_{τ} represents the tau lepton mass. The freeze-out temperature of the stau density $T_{f(\text{ratio})}$ is given by $(m_{\tau} - \delta m)/T_{f(\text{ratio})} \simeq 25$ as in Eq. (9), since the cross section of the exchange process is of the same magnitude as weak processes. Thus $T_{f(\text{ratio})}$ hardly depends on δm . In contrast, the ratio of the number density between stau and neutralino depends on δm according to

Eq. (13), $n_{\tilde{\tau}}/n_{\tilde{\chi}} \sim \exp(-\delta m/T)$, since they follow the Boltzmann distribution before their freeze-out. Thus, the relic density of stau strongly depends on δm .

Here, we comment on the dependence of the stau relic density $n_{\tilde{\tau}^-}$ on other parameters such as $m_{\tilde{\tau}}$, θ_{τ} , and γ_{τ} . The number density of the negatively charged stau is expressed in terms of the total relic density N by

$$n_{\tilde{\tau}^-} = \frac{N}{2(1 + e^{\delta m/T_{f(\text{ratio})}})}. \quad (23)$$

Here, the freeze-out temperature $T_{f(\text{ratio})}$ hardly depends on these parameters. This is because the cross section of the exchange processes are changed by these parameters at most by factors but not by orders of magnitudes, and the $T_{f(\text{ratio})}$ depends logarithmically on $\langle \sigma v \rangle$ as shown in Eq. (9). On the other hand, the total relic density N is proportional to $m_{\tilde{\tau}}$ as in Eq. (22). The value of N is also affected by the left-right mixing θ_{τ} as seen in Fig. 2 since the annihilation cross section depends on this parameter. In contrast, γ_{τ} scarcely affects the relic density, since this parameter appears in the annihilation section through the cross terms of the contributions from the left-handed stau and the right-handed one, and such terms always accompany the suppression factor of $m_{\tau}/m_{\tilde{\tau}}$ compared to the leading contribution. Thus the relic number density of stau $n_{\tilde{\tau}}$ strongly depends on $m_{\tilde{\tau}}$ and θ_{τ} while scarcely depends on γ_{τ} .

We comment on the generality of our method to calculate the density of exotic heavy particles that coannihilate with other (quasi)stable particles: we calculate the total number density of these particles and then calculate the ratio among them by evaluating the exchange processes such as Eq. (10). This method of calculation can be found versatile in various scenarios including the catalyzed BBN and the exotic cosmological structure formation [31–33].

C. Long-lived stau and BBN

After the number density of stau freezes out, stau decays according to its lifetime [3], or forms a bound state with a nuclei in the BBN era. Their formation rate has been studied in literatures [14, 16, 17]. The bound states modify the predictions of SBBN, and make it possible to solve the ^7Li problem via internal conversion processes in the bound state [14–16].

In Fig. 4 we show parameter regions that are consistent with the observed abundances of the DM and of the light elements. We calculate the relic density of stau by varying the value of δm with the values of $m_{\tilde{\tau}} = 350$ GeV, $\sin \theta_{\tau} = 0.8$, and $\gamma_{\tau} = 0$. With these parameters, the allowed region is shown inside the dotted oval. We see that there are allowed regions at $Y_{\tilde{\tau}^-} \sim 10^{-13} - 10^{-12}$ for $\delta m \lesssim 130$ MeV to solve the ^7Li problem at 3σ . On the other hand, it is found that the observational ^6Li to ^7Li ratio excludes $Y_{\tilde{\tau}^-} \gtrsim 10^{-15}$ and $\delta m \lesssim 100$ MeV. We will explain this feature as follows.

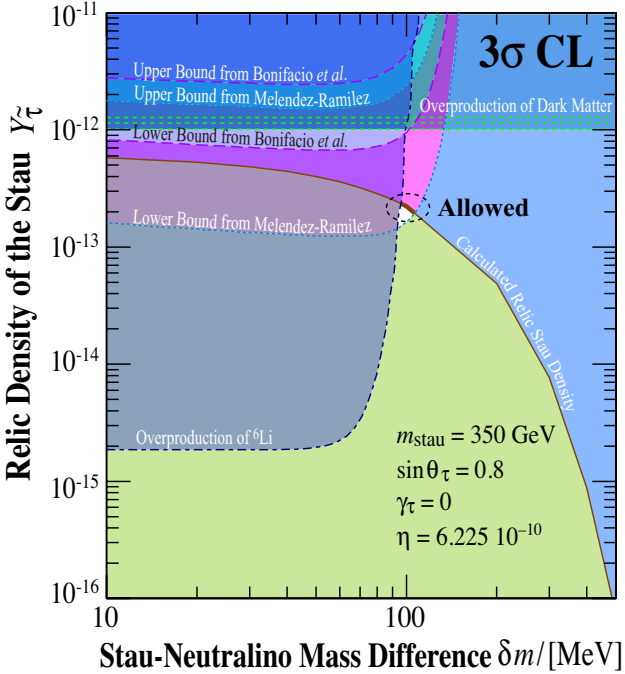


FIG. 4: Parameter regions that are consistent with the observed abundances of the DM and the light elements. Constraints from the observed ${}^7\text{Li}$ abundances are due to Bonifacio *et al.* [36] and Melendez and Ramirez [37]. The calculated relic number density of stau with the indicated parameter is also shown. The top left region is excluded from ${}^6\text{Li}$ overproduction for $Y_{\tilde{\tau}} \gtrsim 10^{-15}$ and $\delta m \lesssim 100$ MeV.

We have adopted following observational abundances of ${}^6\text{Li}$ and ${}^7\text{Li}$. Throughout this subsection, n_i denotes the number density of a particle “ i ”, and observational errors are given at 1σ . For the $n_{{}^6\text{Li}}$ to $n_{{}^7\text{Li}}$ ratio, we use the upper bound [34],

$$(n_{{}^6\text{Li}}/n_{{}^7\text{Li}})_p < 0.046 \pm 0.022 + 0.106, \quad (24)$$

with a conservative systematic error (+0.106) [35]. For the ${}^7\text{Li}$ abundance, we adopt two observational values of the $n_{{}^7\text{Li}}$ to n_{H} ratio. Recently it has been reported to be

$$\log_{10}(n_{{}^7\text{Li}}/n_{\text{H}})_p = -9.90 \pm 0.09, \quad (25)$$

by Ref. [36], and on the other hand, a milder one was also given by Ref. [37],

$$\log_{10}(n_{{}^7\text{Li}}/n_{\text{H}})_p = -9.63 \pm 0.06. \quad (26)$$

In the current scenario ${}^6\text{Li}$ can be overproduced by the scattering of the bound state $({}^4\text{He}\tilde{\tau}^-)$ off the background deuterium through $({}^4\text{He}\tilde{\tau}^-) + \text{D} \rightarrow {}^6\text{Li} + \tilde{\tau}^-$ [4]. The abundance of the nonthermally-produced ${}^6\text{Li}$ through this process is approximately represented by

$$\Delta Y_{\text{Li}} \sim \frac{\langle \sigma v \rangle_{\text{Li}} n_{\text{D}}}{H} Y_{\tilde{\tau}^-}, \quad (27)$$

with $\langle \sigma v \rangle_{\text{Li}}$ the thermal average of the cross section times the relative velocity for this process [38], and n_{D} the number density of deuterium. By using (24), we see that the additional ${}^6\text{Li}$ production is constrained to be $\Delta Y_{\text{Li}} < \mathcal{O}(10^{-21})$. Numerical value of $\langle \sigma v \rangle_{\text{Li}}$ gives $\langle \sigma v \rangle_{\text{Li}} n_{\text{D}}/H \sim \mathcal{O}(10^{-6})$ at $T \sim 10$ keV. Then from (27) it is found that the upper bound on the abundance of stau should be $Y_{\tilde{\tau}^-} \lesssim 10^{-15}$. Because the bound state $({}^4\text{He}\tilde{\tau}^-)$ forms at $T \lesssim 10$ keV, this process is strongly constrained for $\tau_{\tilde{\tau}^-} \gtrsim 10^4$ with $\tau_{\tilde{\tau}^-}$ being the stau lifetime, which corresponds to $\delta m \lesssim 100$ MeV. Note that the ratio $\langle \sigma v \rangle_{\text{Li}} n_{\text{D}}/H$ rapidly decreases as the cosmic temperature decreases, and this nonthermal production of ${}^6\text{Li}$ is much more effective just after formation of the bound state. This is the reason why we can estimate (27) at around 10 keV.

On the other hand, the rates of ${}^7\text{Be}$ and ${}^7\text{Li}$ destruction through the internal conversion [14–16] could be nearly equal to the formation rates of the bound state $({}^7\text{Be}\tilde{\tau}^-)$ and $({}^7\text{Li}\tilde{\tau}^-)$, respectively. This is because the timescale of the destruction through the internal conversion is much faster than that of any other nuclear reaction rates and the Hubble expansion rate. Then the destroyed amount of ${}^7\text{Be}$ (or ${}^7\text{Li}$ after its electron capture) is approximately represented by

$$\Delta Y_{\text{Be}} \sim \frac{\langle \sigma v \rangle_{\text{bnd},7} n_{\text{Be}}}{H} Y_{\tilde{\tau}^-}, \quad (28)$$

where $\langle \sigma v \rangle_{\text{bnd},7} \sim 10^{-2} \text{GeV}^{-2} (T/30\text{keV})^{-1/2} (Z/4)^2 \times (A/7)^{-3/2} (E_{\text{b}}/1350\text{keV})$ is the thermally-averaged cross section times the relative velocity of the bound-state formation for $({}^7\text{Be}\tilde{\tau}^-)$ [16, 17]. We request ΔY_{Be} to become $\sim \mathcal{O}(10^{-20})$ to reduce the abundance of ${}^7\text{Be}$ to fit the observational data. Then the abundance of $\tilde{\tau}^-$ should be the order of $\Delta Y_{\text{Be}} (\langle \sigma v \rangle_{\text{bnd},7} n_{\text{Be}}/H)^{-1} \sim \mathcal{O}(10^{-12})$ with $\langle \sigma v \rangle_{\text{bnd},7} n_{\text{Be}}/H \sim 10^{-8}$ at $T = 30$ keV. Because $\langle \sigma v \rangle_{\text{bnd},7} n_{\text{Be}}/H$ decreases as the cosmic temperature decreases ($\propto T^{1/2}$), the destruction is more effective just after the formation of the bound state. This validates that we have estimated (28) at 30 keV. Therefore the parameter region at around $Y_{\tilde{\tau}^-} \sim 10^{-12}$ and $\delta m \lesssim 130$ MeV is allowed by the observational ${}^7\text{Li}$. Here $\delta m \lesssim 130$ MeV corresponds to $\tau_{\tilde{\tau}^-} \gtrsim 10^3$ s. The case for the destruction of $({}^7\text{Li}\tilde{\tau}^-)$ through the internal conversion is also similar to that of $({}^7\text{Be}\tilde{\tau}^-)$ [14, 15].

Further constraints come from the relic density of the DM, which can be stated in terms of the stau relic density. It is calculated as shown in Fig. 4 for the present values of parameters. Applying all the constraints, we are led to the allowed interval shown by the thick line in the figure.

D. Constraint on parameter space of stau

Finally, we show in Fig. 5 the parameter space in which the calculated abundances of the DM and that of the light elements are consistent with their values from the observations. Here, based on the discussion in previous

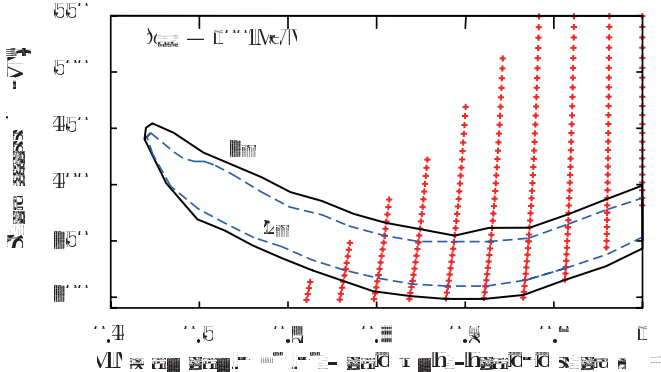


FIG. 5: Parameter space in which the calculated abundances of the DM and that of the light elements are consistent with their values from the observations. Parameter region surrounded by black solid (blue dashed) line shows the allowed region from the WMAP observation at the 3σ (2σ) level [1]. Red crisscross points show the parameters which is consistent with observational abundances for the light elements including ${}^7\text{Li}$ at 3σ level.

subsection, we took $\delta m = 100$ MeV. Parameter region surrounded by black solid (blue dashed) line is allowed by the relic abundance of the DM from the WMAP observation at the 3σ (2σ) level [1], which corresponds to $0.0913 \leq \Omega_{\text{DM}}h^2 \leq 0.1285$ ($0.0963 \leq \Omega_{\text{DM}}h^2 \leq 0.1213$). Red crisscross points show the parameters which are consistent with the observational abundances for the light elements including ${}^7\text{Li}$, where the observational ${}^7\text{Li}$ abundance is yielded by literature [37].

The abundance of the light elements constrains the parameter space due to the following reasons. First, the region where the stau mass is less than 300 GeV is excluded since the relic density becomes too small to destruct ${}^7\text{Li}$ sufficiently. Next, the top-left region of the figure is excluded since the lifetime of stau becomes too long and hence overproduces ${}^6\text{Li}$ through the catalyzed fusion [4]. Indeed, the lifetime of stau gets longer as its mass gets heavier due to the small phase space of the final state [3]. On the other hand, its lifetime gets shorter as the left-right mixing angle increases in the present parameter space [3]. As a result, the final allowed region becomes as shown by the red crisscrosses in Fig. 5.

The black solid curve and the blue dashed curve are the constraints from the relic abundance of the DM as discussed in subsection III A. Note that the relic abundance is insensitive to the mass difference δm for $\delta m \ll m_{\tilde{\chi}}$. Combination of the constraints on the abundance of the light elements and of the DM strongly restricts the allowed region and leads to $\delta m \simeq 100$ MeV, $m_{\tilde{\tau}} = (300 - 400)$ GeV, and $\sin \theta_{\tau} = (0.65 - 1)$. In Fig. 4, these parameter values correspond to the white triangular region below the allowed region (thick line). Our model can thus provide a handle to the mixing angle, which has few experimental signals, once the value of $m_{\tilde{\tau}}$ is determined.

IV. SUMMARY AND DISCUSSION

We have studied the evolution of stau number density in the MSSM coannihilation scenario, in which the LSP and the NLSP are the lightest neutralino and the lighter stau, respectively, and have a small mass difference $\delta m \lesssim \mathcal{O}(1\text{GeV})$. In this case, stau can survive until the BBN era, and provide additional nucleosynthesis processes. It is therefore necessary to see how large the relic density of stau is at the BBN era.

We have shown the Boltzmann equations for the calculation of the relic number density of stau, and have found that the number density of stau continues to evolve through the exchange processes Eq.(10), even after the relic abundance of the DM is frozen out. Thus, we need to calculate the stau relic density by a two-step procedure. In the first step, we calculate the total abundance of stau and neutralino, which corresponds to the relic abundance of the DM. The total abundance is controlled only by pair annihilation processes of the supersymmetric particles. In the second step, we calculate the ratio of the stau number density to the total number density of stau and neutralino, which is governed only by the exchange processes. We have calculated the relic density of stau at the BBN era by solving the Boltzmann equations numerically. The freeze-out temperature $T_{f(\text{ratio})}$ is determined by $(m_{\tau} - \delta m)/T_{f(\text{ratio})} \simeq 25$ and the relic density of stau are given by Eq. (23). Thus it becomes larger as the mass difference between stau and neutralino gets smaller. Our method of calculation is generally applicable to obtain the density of exotic heavy particles that coannihilate with other (quasi)stable particles: we calculate the total number density of these particles and then calculate the ratio among them by evaluating the exchange processes such as Eq. (10). This method of calculation can be found versatile in various scenarios including the catalyzed BBN and the exotic cosmological structure formation.

At the BBN era, the long-lived stau form bound states with nuclei, and provide exotic nucleosynthesis processes. One of them is the internal conversion process, which offers a possible solution to the ${}^7\text{Li}$ problem. Applying the calculated relic density of stau, we have calculated the primordial abundance of light elements including these exotic processes. We have found the parameter space consistent with both of the calculational results and the observations for the relic abundance of the DM and the light elements abundance including ${}^7\text{Li}$. We have shown a prediction for the values of the parameters relevant to stau and neutralino, which is shown in Fig. 5. Consistency between the theoretical prediction and the observational result, both of the DM abundance and the light elements abundance requires $\delta m \simeq 100$ MeV, $m_{\tilde{\tau}} = (300 - 400)$ GeV, and $\sin \theta_{\tau} = (0.65 - 1)$.

Acknowledgments

The work of K. K. was supported in part by PPARC Grant No. PP/D000394/1, EU Grant No. MRTN-CT-2006-035863, the European Union through the Marie Curie Research and Training Network “UniverseNet,” MRTN-CT-2006-035863, and Grant-in-Aid for Scientific research from the Ministry of Education, Science, Sports, and Culture, Japan, No. 18071001. The work of J. S.

was supported in part by the Grant-in-Aid for the Ministry of Education, Culture, Sports, Science, and Technology, Government of Japan (No. 20025001, 20039001, and 20540251). The work of T. S. was supported in part by MEC and FEDER (EC) Grants No. FPA2005-01678. The work of M. Y. was supported in part by the Grant-in-Aid for the Ministry of Education, Culture, Sports, Science, and Technology, Government of Japan (No. 20007555).

[1] J. Dunkley *et al.* [WMAP Collaboration], *Astrophys. J. Suppl.* **180** (2009) 306

[2] K. Griest and D. Seckel, *Phys. Rev. D* **43**, 3191 (1991).

[3] T. Jittoh, J. Sato, T. Shimomura and M. Yamanaka, *Phys. Rev. D* **73** (2006) 055009

[4] M. Pospelov, *Phys. Rev. Lett.* **98** (2007) 231301

[5] M. Kaplinghat and A. Rajaraman, *Phys. Rev. D* **74**, 103004 (2006).

[6] R. H. Cyburt, J. Ellis, B. D. Fields, F. Luo, K. A. Olive and V. C. Spanos, arXiv:0907.5003 [astro-ph.CO].

[7] M. Kamimura, Y. Kino and E. Hiyama, *Prog. Theor. Phys.* **121** (2009) 1059

[8] M. Kusakabe, T. Kajino, T. Yoshida, T. Shima, Y. Nagai and T. Kii, *Phys. Rev. D* **79** (2009) 123513

[9] M. Pospelov, J. Pradler and F. D. Steffen, *JCAP* **0811** (2008) 020

[10] K. Jedamzik, *JCAP* **0803** (2008) 008

[11] M. Kawasaki, K. Kohri and T. Moroi, *Phys. Lett. B* **649**, 436 (2007); M. Kawasaki, K. Kohri, T. Moroi and A. Yotsuyanagi, *Phys. Rev. D* **78** (2008) 065011

[12] J. Pradler and F. D. Steffen, *Phys. Lett. B* **666** (2008) 181

[13] K. Jedamzik, *Phys. Rev. D* **77** (2008) 063524

[14] T. Jittoh, K. Kohri, M. Koike, J. Sato, T. Shimomura and M. Yamanaka, *Phys. Rev. D* **76** (2007) 125023

[15] T. Jittoh, K. Kohri, M. Koike, J. Sato, T. Shimomura and M. Yamanaka, *Phys. Rev. D* **78** (2008) 055007

[16] C. Bird, K. Koopmans and M. Pospelov, *Phys. Rev. D* **78** (2008) 083010

[17] K. Kohri and F. Takayama, *Phys. Rev. D* **76** (2007) 063507

[18] S. Bailly, K. Jedamzik and G. Moultsaka, arXiv:0812.0788 [hep-ph]; S. Bailly, K. Y. Choi, K. Jedamzik and L. Roszkowski, *JHEP* **0905**, 103 (2009).

[19] R. H. Cyburt, B. D. Fields and K. A. Olive, arXiv:0808.2818 [astro-ph].

[20] F. Spite and M. Spite, *Astron. Astrophys.* **115** (1982) 357.

[21] R. H. Cyburt and B. Davids, *Phys. Rev. C* **78** (2008) 064614

[22] O. Richard, G. Michaud and J. Richer, *Astrophys. J.* **619**, 538 (2005)

[23] A. J. Korn *et al.*, *Nature* **442** (2006) 657

[24] J. Melendez *et al.*, arXiv:0910.5845 [astro-ph.SR].

[25] K. Lind, F. Primas, C. Charbonnel, F. Grundahl and M. Asplund, arXiv:0906.2876 [astro-ph.SR].

[26] J. Edsjo and P. Gondolo, *Phys. Rev. D* **56** (1997) 1879

[27] C. F. Berger, L. Covi, S. Kraml and F. Palorini, *JCAP* **0810**, 005 (2008)

[28] G. Belanger, F. Boudjema, A. Pukhov and A. Semenov, *Comput. Phys. Commun.* **180** (2009) 747

[29] T. Falk, K. A. Olive and M. Srednicki, *Phys. Lett. B* **339** (1994) 248

[30] E. W. Kolb and M. S. Turner, *The Early Universe* (Addison-Wesley, Redwood City, 1990).

[31] K. Sigurdson and M. Kamionkowski, *Phys. Rev. Lett.* **92**, 171302 (2004)

[32] S. Profumo, K. Sigurdson, P. Ullio and M. Kamionkowski, *Phys. Rev. D* **71**, 023518 (2005)

[33] K. Kohri and T. Takahashi, *Phys. Lett. B* **682**, 337 (2010)

[34] M. Asplund, D. L. Lambert, P. E. Nissen, F. Primas and V. V. Smith, *Astrophys. J.* **644** (2006) 229

[35] J. Hisano, M. Kawasaki, K. Kohri, T. Moroi and K. Nakayama, *Phys. Rev. D* **79**, 083522 (2009).

[36] P. Bonifacio *et al.*, arXiv:astro-ph/0610245.

[37] J. Melendez and I. Ramirez, *Astrophys. J.* **615**, L33 (2004).

[38] K. Hamaguchi *et al.*, arXiv:hep-ph/0702274.